Mechanical milling effect on the structural and magnetic properties of sintered $La_{0.67}Sr_{0.33}MnO_3$

Itegbeyogene P. Ezekiel[1], **Thomas Moyo and Sanele Dlamini**
School of Chemistry and Physics, University of KwaZulu-Natal, P/Bag X5401, Durban 4000, South Africa

E-mail: itegbeyogene@gmail.com

Abstract. We report structural and temperature dependence of magnetization properties of the as-sintered and milled $La_{0.67}Sr_{0.33}MnO_3$ oxides. The refined X-ray diffraction data show that all samples are single phase and crystallize in rhombohedral symmetry. The crystallite sizes decreased from 46 nm to 11 nm after milling the as-sintered sample for 1, 3, 6 and 12 hours. The surface morphology of the samples shows significant changes at the surface of all the samples. The saturation magnetization M_S is observed to follow Bloch's law. M_S decreases from 52 emu/g to 7 emu/g at 300 K and from 80 emu/g to 40 emu/g at 2 K due to particle size reduction. We use core-shell model to investigate changes in M_S as function of particle size and estimate a dead layer thickness of the nanoparticles to be about 0.96 nm. The results show increased coercive fields with reduction in temperature and particle size. The coercive field at 2 K show a significant increase from 170 Oe to 870 Oe in the sample milled for 12 hours. We also report the effects of zero field cooling and field cooling on the magnetisation of the samples.

1. Introduction

The possible application of perovskite manganites in solid-state refrigeration and their colossal magnetoresistance have contributed to several studies of these materials [1-3]. The double exchange interaction that exists between the Mn^{3+}-O-Mn^{4+} bonds in the manganite structure of $A_{1-x}B_xMnO_3$ where A is a rare-earth element and B is divalent element [4-6], influences the properties. In particular, La-Sr-manganites have shown promising potential applications near room temperature. The $La_{1-x}Sr_xMnO_3$ perovskites, at the composition $x = 0.33$ has attracted much attention because its Curie temperature is about 370 K and has a large magnetic moment [1]. This makes it a good candidate for magnetocaloric effect applications near room temperature. A study of $La_{0.9}Sr_{0.1}MnO_3$ synthesized by the citrate-gel method reveals how the magnetic properties of these materials can significantly change due to surface effects. The sample initially had a Curie temperature T_C of 250 K, which decreased with increase in grain size [3]. The synthesis process and surface spins appear to also play important roles in determining the final properties. The interest in this study is to investigate the particle size and surface effects on the structural and magnetic properties of mechanically milled $La_{0.67}Sr_{0.33}MnO_3$ perovskites initially synthesized by solid-state reaction process.

2. Experimental details

$La_{0.67}Sr_{0.33}MnO_3$ was synthesised by the pre-sintering of a pellet of a well-mixed high purity La_2O_3, SrO and MnO_2 powders at 1200 °C for 15 hours. The pellet was ground in an agate mortar and pestle into powder and another pellet was prepared for further sintering at 1350 °C for 15 hours. This is a double sintering process. We re-ground the final pellet in an agate mortar and pestle, denoted as sample S0. The effects of mechanical milling on the magneto-structural properties of S0 was studied on samples S1, S3, S6 and S12 after S0 was mechanically milled in a Retsch PM 400 planetary ball mill at a ball to mass ratio of 20:1 and speed of 250 rpm for 1, 3, 6, and 12 hours respectively. Appropriate amounts of samples about 0.5 g were available for X-ray diffraction (XRD) with a CuKα radiation source. A Zeiss ultra plus high-resolution scanning electron microscope (HRSEM) was used to study the surface morphology. Each sample was held fixed in a Perspex cone sample holder by a piece of cotton wool for the magnetization measurements in a Cryogenic Ltd 5 Tesla mini cryogen free measurement system. This avoids torque during the measurements.

3. Results and discussion

The XRD patterns of the samples shown in Figure 1 were analysed using Fullprof-Suite [1]. All the samples have rhombohedral structure that belongs to the space group $R3C$ [3]. The values of the refined lattice parameters and the cell volumes presented in Table 1 are in close agreement with reported values [1, 6]. The significant shift observed in the S12 pattern towards higher values of 2θ is associated with a reduction in lattice parameters caused by high surface deformation and strain due to prolonged milling. Figure 2 shows estimates of the strain and average crystallite sizes from the Williamson-Hall plot [7] and the Scherrer formula [8] respectively. High-energy mechanical ball milling is an effective technique for achieving reduction in particle sizes due to the grinding effect of the balls [9]. Figure 2 shows the results. The slight increase in the crystallite size for S12 appears to be due to a thermal annealing effect because of prolonged high-energy ball milling. In this case, further particle size reduction does not occur due to limited sizes of the grinding balls but instead the mechanical energy goes into heating the sample. This caused sample S12 to exhibit a different trend.

The HRSEM images in Figure 3 show the milling effect on the surface morphology of the samples. The images clearly show a variation in the surface texture with a more compacted surface for S12. Considering the high percentage of atoms at the surface of nanomaterials [10], we expect a modification of the magnetic properties of the samples due to such variations. Nanoparticles usually have high percentage of its atoms at the surface of the core [10]. Therefore, as the size of the core of the nanoparticle reduces, the surface to core volume ratio increases.

Figures 4 and 5 show magnetic hysteresis loops measured at 300 K and 2 K respectively. The loops are typical of ferromagnetic order having a sigmoidal shape with noticeable hysteresis as shown in Figure 6. The coercive field $H_C = \left|H_{C1} + H_{C2}\right|/2$ was estimated from the hysteresis loops where H_{C1} and H_{C2} are the values of the negative and positive coercive fields respectively [11]. Figure 7 shows the temperature T dependence of the saturation magnetization M_S which were deduced by using the law of approach to saturation [12]. The M_S dependence on T in Figure 7 follows the modified Bloch's law $M_S(T) = M_S(0)\left(1 - \frac{T}{T_0}\right)^{\beta}$ [12] with fit parameters given in Table 2. The characteristic temperature T_0 where the magnetization becomes zero decreases continuously as a function of milling time. The Bloch's exponent β values are in the range of reported values [13]. The solid line in the H_C dependence on T is a guide to the eye. The decrease in T_0 and M_S is attributed

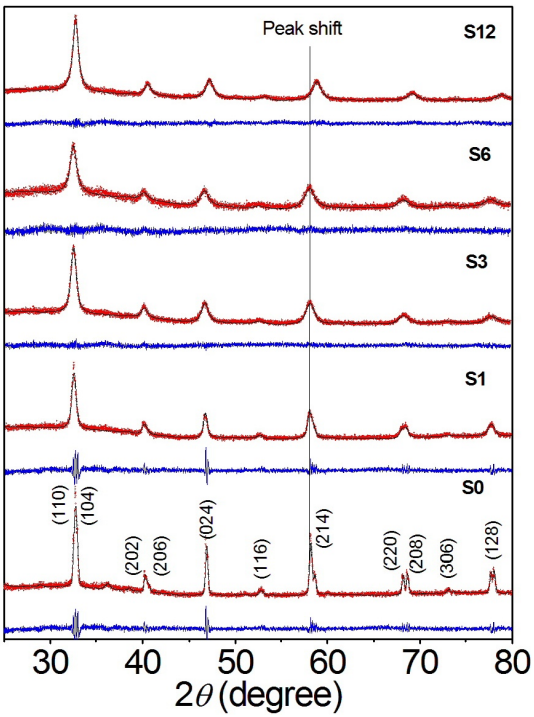

Figure 1. Refined XRD patterns for as-sintered sample (S0) and milled samples for 1, 3, 6 and 12 hours.

Table 1. Lattice parameters a, b, c, cell volume V and goodness of χ^2 as obtained from Rietveld refinements of as-sintered sample S0 and the milled samples.

	$a = b$ (Å) ±0.006	c (Å) ±0.002	V (Å^3) ±0.079	χ^2
S0	5.499	13.344	349.448	3.32
S1	5.503	13.366	350.559	2.41
S3	5.495	13.417	350.875	2.25
S6	5.497	13.469	352.424	2.39
S12	5.485	13.412	349.383	2.18

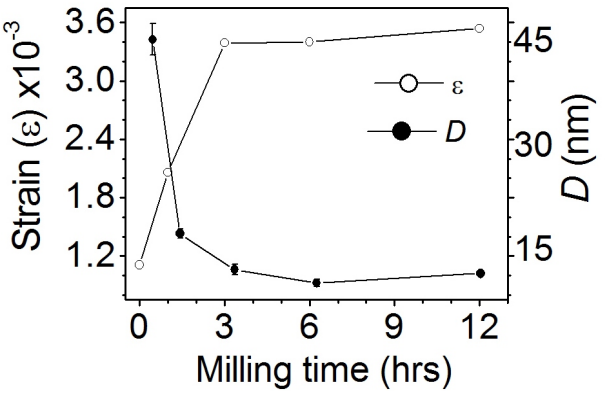

Figure 2. Average crystallite size D and the strain ε as a function of milling time.

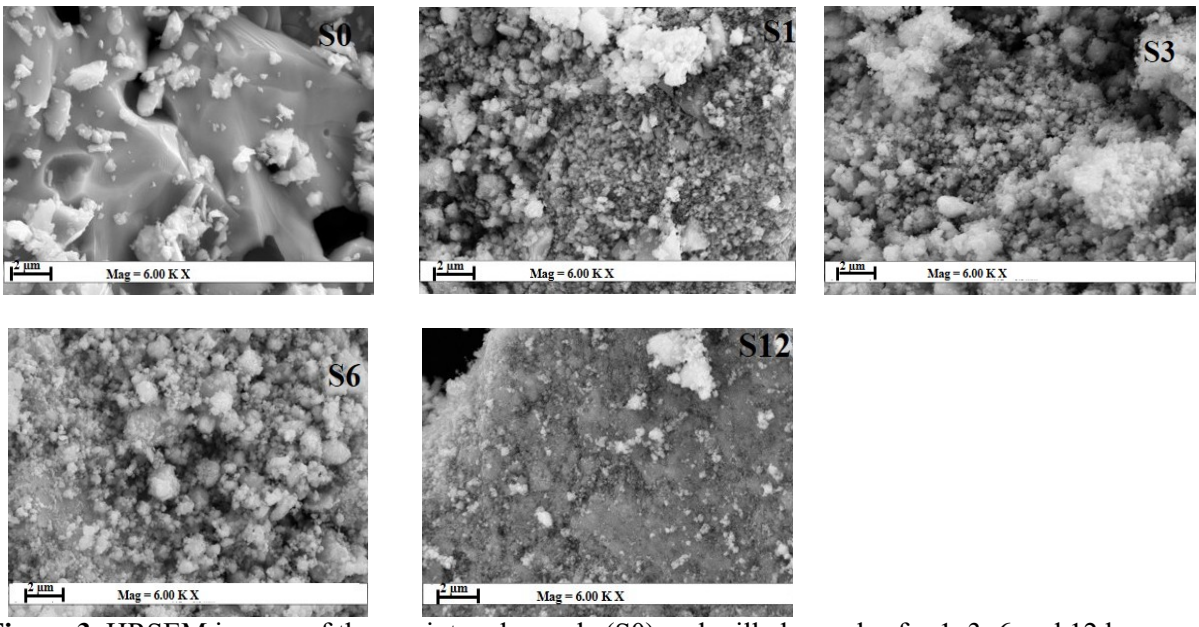

Figure 3. HRSEM images of the as-sintered sample (S0) and milled samples for 1, 3, 6 and 12 hours.

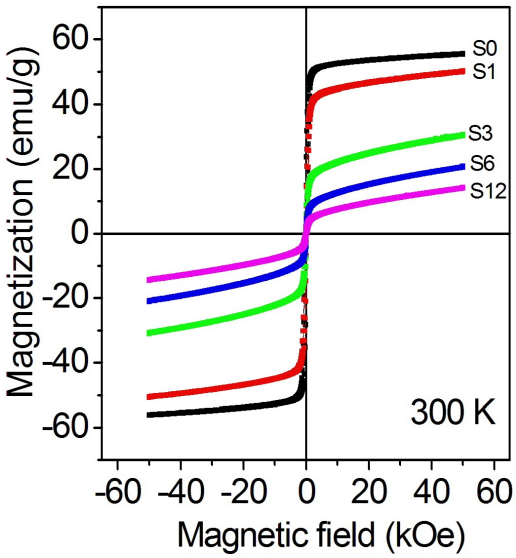

Figure 4. Magnetic hysteresis loops measured at 300 K.

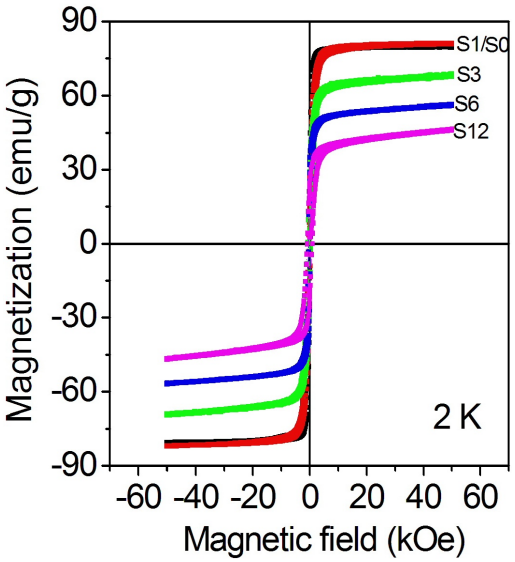

Figure 5. Magnetic hysteresis loops measured at 2 K.

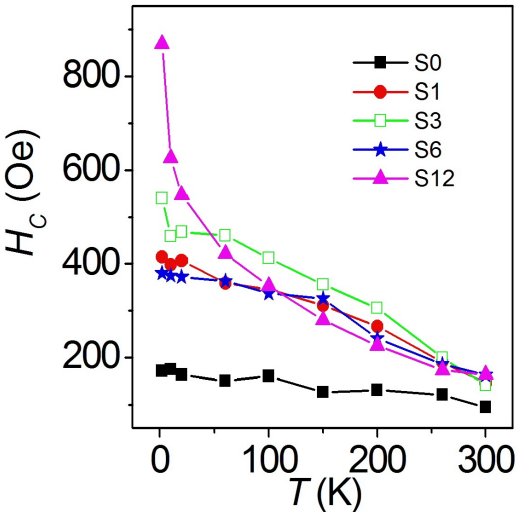

Figure 6. Temperature dependence of coercive field H_C.

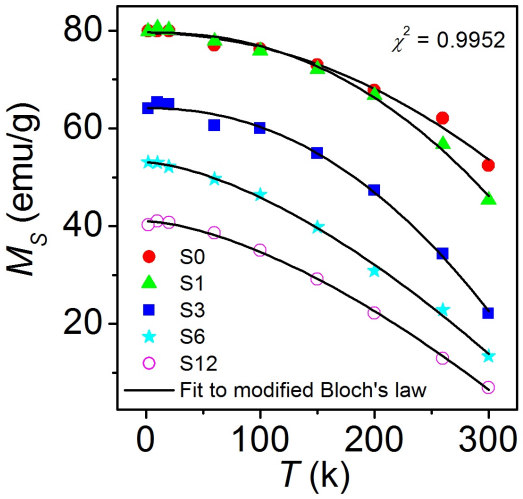

Figure 7. Temperature dependence of saturation magnetization, M_S.

Table 2. Saturation magnetization $M_S(0)$, characteristic temperature T_0, Bloch's exponent β and the goodness of fit χ^2.

Sample	$M_S(0)$ (emu/g) ±0.5	T_0 (K) ±14	β ±0.1	χ^2
S0	79	522	2.0	0.989
S1	79	440	2.3	0.995
S3	64	367	2.2	0.995
S6	53	365	1.5	0.998
S12	41	335	1.6	0.999

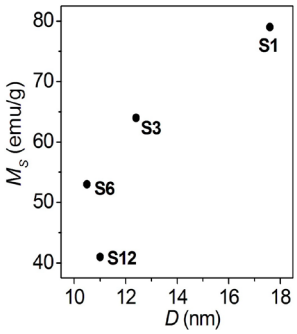

Figure 8. Dependence of saturation magnetization on the crystallite size.

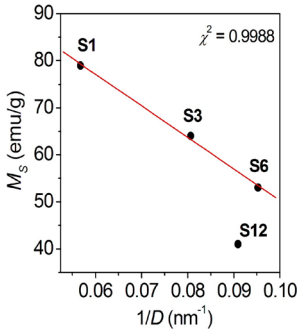

Figure 9. A fit to estimate M_S(bulk) and the thickness dead layer d.

to a disordered surface spin called the "magnetic dead layer" as earlier shown in the surface morphology changes in the HRSEM and the decrease in particle size as measured from the XRD results. This can best be described by the core shell model [1, 14]. The shell (layer) consists of disordered moments with an ordered core. The magnetization decreases as the milling time increases. This explains the decrease in M_S as the core decreases as shown in Figure 8. The dead layer thickness d = 0.96±0.01 nm is estimated from the dependence of M_S on the inverse of crystallite size D using formula $M_S = M_S(\text{bulk})\left[1-\frac{6d}{D}\right]$ [1, 14, 15]. Figures 9 shows a very strong correlation ($\chi^2 = 0.9988$) between M_S and D^{-1} for samples S1, S3 and S6. The M_S(bulk) was estimated be 117±3 emu/g. The sample S12 appears not to be part of this set consistent with XRD data in Figure 1. For S1-S6, the thickness of the layer does not significantly change [1] with the milling time. However, the degree of disorder in the dead layer could vary.

Figure 10 shows the zero-field cooled (ZFC) and field cooled (FC) magnetizations of samples S0, S1, S6 and S12 which are used to investigate changes in the blocking temperature T_B and the irreversibility temperature T_{irr}. The results show significant differences between ZFC and FC magnetizations. The step in the ZFC and FC at 43 K for S0 is due to the inhomogeneous nature of the ferromagnetic clusters. This decreases in the FC curve of S1 and disappears completely on further milling. Below the freezing temperature of T_f = 43 K, the moments are frozen therefore the FC curve remains unchanged. In Figure 11, T_B significantly drops from 280 K for S0 to 122 K for S12, while T_{irr} drops from 312 K to 256 K. This shows strong dependence of T_B and T_{irr} on particle size.

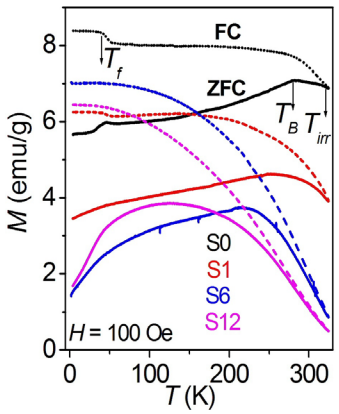

Figure 10. ZFC-FC magnetization curves.

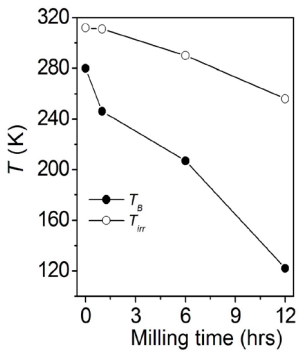

Figure 11. Blocking temperature T_B and irreversibility temperature, T_{irr}.

4. Conclusions

We have investigated the particle size and surface effects on the structural and magnetic properties of double sintered and subsequently milled samples of $La_{0.67}Sr_{0.33}MnO_3$ oxides. The XRD data shows all samples in single phase and crystallized in rhombohedral structure. The crystallite sizes decreased as a function of milling time except for the S12 sample, which increased slightly due to suspected thermal annealing effect caused by prolonged milling. In this case, particle size reduction appears less effective at the lowest particle size. In all the samples, the temperature dependence of the saturation magnetization M_S follows the Bloch's law. The evolution of M_S with reduction in particle size follows the core-shell model except for the S12 sample, which appears not to be part of the set. Using the core-shell model, we have determined the thickness of the disordered surface layer for milled samples S1, S3 and S6 to be 0.96 nm. All the samples show significant ZFC and FC effects, which we attribute to ferromagnetic clusters at the core surrounded by disordered surface layers.

Acknowledgments

The authors are thankful to the National Research Foundation of South Africa and the University of KwaZulu-Natal for research grants.

References

[1] Rostamnejadi A, Venkatesan M, Kameli P, Salamati H and Coey J M D 2011 *J. Magn. Magn. Mater*. **323** 2214.
[2] Giri S K, Dasgupta P, Poddar A, Nigam A K and Nath T K J 2014 *J. Alloys Comp*. **582** 609.
[3] Baaziz H, Tozri A, Dhahri E and Hilil E K 2015 *Ceramics Int*. **41** 2955.
[4] Skini R, Khlifi M, Dhahri E and Hilil E K 2014 *J. Supercond. Nov. Magn.* **27** 247.
[5] Ho T A, Lim S H, Tho P T, Phan T L and Yu S C 2017 *J. Magn. Magn. Mater* **426** 18.
[6] Rocco D, Coelho A A, Gama S and Santos M C 2013 *J. Appl. Phys*. **113** 113907.
[7] Zak A, Khorsand W H, Majid Abd, Abrishami M E and Yousefi R 2011 *Sol. Stat. Sci.* **13** 251.
[8] Abdallah H M I, Moyo T, Itegbeyogene E P and Osman N S E 2014 *J. Magn. Magn. Mater*. **365** 83.
[9] Yadav T P, Yadav R M and Singh D P 2012 *J. Nanosci. Nanotechnol*. **2(3)**, 22.
[10] Kodama R H 1999 *J. Magn. Magn. Mater*. **200** 359.
[11] Ramudu M and J Gerhard 2013 *J. Appl. Phys. Lett*.**102** 232406.
[12] Andreev S V, Bartashevich M I, Pushkarsky V I, Maltsev V N, Pamyatnykh L A, Tarasov E N, Kudrevatykh N V and Goto T 1997 *J. Alloys Comp*. **260** 196.
[13] Maaz K, Mumtaz A, Hasanain S K and Bertino M F 2010 *J. Magn. Magn. Mater.* **322** 2199.
[14] Sarkar T, Raychaudhuri A K, Bera A K and Yusuf S M 2010 *New J. Phys*. **12** 123026.
[15] Vázquez-Vázquez C, López-Quintela M A, Buján-Núñez M C and Rivas J 2011 J. *Nanopart. Res*. **13** 1663.